0.8. In fact, the error is less than 1 percent for $\delta = 0.95$. On the other hand, (33) is accurate for small values ρ. These expansions also give the limiting behavior of the capacitance as δ and ρ approach zero.

APPENDIX

The expansion for C_0 in terms of δ given in (28) requires more terms in the expansion for K'/K in terms of k than are generally known. For future possible interest, the first 12 terms in this expansion are

$$\pi\frac{K'}{K} = \log\left(\frac{16}{k^2}\right) - \frac{1}{2}\left[k^2 + \frac{13}{32}k^4 + \frac{23}{96}k^6 + \frac{2701}{16384}k^8 + \frac{5057}{40960}k^{10} + \frac{76715}{786432}k^{12} + \frac{146749}{1835008}k^{14} + \frac{144644749}{2147483648}k^{16} + \frac{279805685}{4831838208}k^{18} + \frac{4346533901}{85899345920}k^{20} + \frac{8465644159}{188978561024}k^{22} + \cdots\right]. \quad (34)$$

The method used to determine these coefficients is detailed in Riblet [3, p. 665]. The identity [4, p. 73]

$$\frac{K(k_0)}{K'(k_0)} = 2\frac{K(k_1)}{K'(k_1)} \quad (35)$$

when

$$k_0 = \frac{2\sqrt{k_1}}{1+k_1}$$

can also be used to find them as the solution of a set of linear equations if an expansion for K'/K of the required form is substituted in (35). In fact, it is the complete agreement between the decimal values obtained from these independent procedures which provides the author with the confidence to present these computer-generated rational values.

REFERENCES

[1] F. Bowman, "Notes on two-dimensional electric field problems," *Proc. London Math. Soc.*, ser. 2, vol. 41, pp. 271–277, 1935.

[2] P. A. A. Laura and L. E. Luisoni, "Approximate determination of the characteristic impedance of the coaxial system consisting of a regular polygon concentric with a circle," *IEEE Trans. Microwave Theory Tech.*, vol. MTT-25, pp 160–161, Feb. 1977.

[3] H. J. Riblet, "Two limiting values of the capacitance of symmetrical rectangular coaxial strip transmission line," *IEEE Trans. Microwave Theory Tech.*, vol. MTT-29, pp. 661–666, July 1981.

[4] F. Bowman, *Introduction to Elliptic Functions with Applications*. New York: Dover, 1961, pp. 56–69

A Coplanar Probe to Microstrip Transition

DYLAN F. WILLIAMS, MEMBER, IEEE,
AND TOM H. MIERS, MEMBER, IEEE

***Abstract*—A transition between a coplanar probe and a microstrip transmission line is reported. The transition is significant in that it does not require substrate via holes. A set of microstrip impedance standards were developed for the purpose of de-embedding the transition. The transition is suitable for measuring the S parameters of a number of low-cost monolithic microwave integrated circuits with coplanar probes.**

Manuscript received October 3, 1987; revised February 12, 1988.

The authors are with Ball Aerospace Systems Division, P.O Box 1062, Boulder, CO 80306-1062.

IEEE Log Number 8821226.

I. INTRODUCTION

The S parameters of planar microwave devices may be measured accurately and efficiently with coplanar probes [1]. Using coplanar probes to measure the S parameters of monolithic microwave integrated circuits (MMIC's) based on microstrip transmission lines is difficult, however, because the ground plane of the microstrip transmission lines is not easily contacted by the coplanar probe. Moniz [2] and Harvey [3] have used plated substrate via holes for this purpose, but the difficult processing required to form these via holes inevitably raises the circuit fabrication cost and lowers the yield. For these reasons it is often desirable to use a transition which does not require substrate via holes, especially if the circuit to be fabricated does not require via hole grounding.

In this work a transition between a coplanar probe and a microstrip transmission line which does not require substrate via holes and which is suitable for performing S parameter measurements of microstrip MMIC's is described. The method used to de-embed and unterminate the transition is discussed and the S parameters of the transition deduced from this procedure are presented. The accuracy of the de-embedded measurements is estimated.

II. COPLANAR PROBE TO MICROSTRIP TRANSITION

The coplanar probe to microstrip transition investigated in this work is shown in Fig. 1. The center signal pad on the coplanar probe contacts the microstrip line into which the signal is launched. The outer two ground pads on the coplanar probe contact the microstrip radial stub near its center. The microstrip radial stub provides a low impedance between the microstrip ground plane and the coplanar probe ground contacts. (Other stub types could be used but would exhibit a more narrow band performance.)

If the fringing fields at the stub edges can be ignored, the electrical reactance X between the probe ground and the microstrip ground can be estimated from the formulas given by Atwater [4]:

$$X = (h/2\pi r_1)\, Z_0(r_1)(360/\theta)\cos(\theta_1 - \Phi_2)/\sin(\Phi_1 - \Phi_2) \quad (1)$$

where

$$\tan(\theta_1) = N_0(kr_1)/J_0(kr_1)$$

$$\tan(\Phi_i) = -J_1(kr_i)/N_1(kr_i) \qquad (i = 1,2)$$

$$Z_0(r_1) = (120\pi/\sqrt{\epsilon_{re}})\left[J_0^2(kr_1) + N_0^2(kr_1)\right]^{1/2} \cdot \left[J_1^2(kr_1) + N_1^2(kr_1)\right]^{-1/2}$$

$$k = 2\pi\sqrt{\epsilon_{re}}/\lambda_0$$

and θ is the angle subtended by the stub, ϵ_{re} is the effective dielectric constant (which may be approximated by the substrate relative dielectric constant ϵ_r for large θ), h is the substrate thickness, λ_0 is one free-space wavelength, $J_i(x)$ and $N_i(x)$ are

0018-9480/88/0700-1219$01.00 ©1988 IEEE

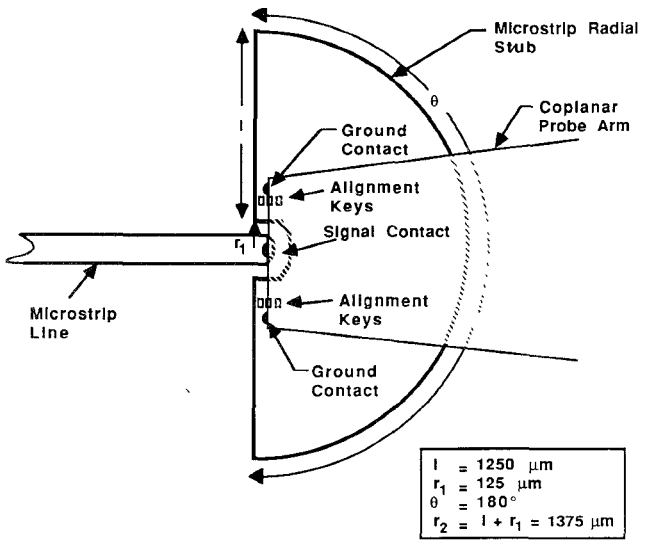

Fig 1. The coplanar probe to microstrip transition investigated in this work is shown from above. The 180° radial stub provides a low impedance between the microstrip ground plane and the top surface of the substrate. The outer two (ground) coplanar probe pads contact the radial stub near its vertex The microstrip line is contacted by the center (signal) coplanar probe pad. The alignment holes on the radial stub aid in achieving repeatable probe placement

Bessel functions of the first and second kinds of the ith order, r_1 is the inner radius, r_2 is the stub outer radius, and $l = r_2 - r_1$ as defined in Fig. 1. (The quantity r_1 is defined for a circular inner stub contour. Since the inner stub contour used in this work was not circular, the distance from the center of the stub to the leftmost vertex, as drawn in Fig. 1, was used in place of r_1. This approximation is reasonable given the approximations already made in deriving (1).) Atwater [4] also shows that if fringing fields can be neglected, the stub angle is large, and the stub inner radius r_1 is small compared with a wavelength, the lowest stub impedance is achieved by a stub of length [4]

$$l \approx \lambda_0/(2\pi\sqrt{\epsilon_r}). \tag{2}$$

It is easy to show that, under the same assumptions used to derive (2), the stub reactance becomes infinite when

$$l \approx 3.832\lambda_0/(2\pi\sqrt{\epsilon_r}). \tag{5}$$

(The frequencies at which the stub impedance is zero and nearly infinite are actually somewhat lower than calculated here because of fringing effects, which were not taken into account in (1), (2), and (3).)

For any given frequency of operation, the optimum stub has a length given approximately by (2), since the impedance of the stub is both low and insensitive to the substrate thickness at that length. (Insensitivity to substrate thickness can be an important advantage when making measurements on many wafers of differing thicknesses.)

At the frequency at which (3) is satisfied, the coplanar probe ground and the microstrip ground plane decouple. Equation (3) thus determines approximately the highest frequency at which the stub may be used.

From (1) it can be seen that the stub reactance is inversely related to the stub angle θ. The bandwidth of the stub, defined as the frequency range for which the impedance of the radial stub is below some threshold impedance, thus increases as the stub angle θ increases. A stub angle θ of 180° results in a large bandwidth. A larger stub angle was deemed undesirable as the transition would consume too large a surface area, an important consideration in GaAs MMIC's, while not greatly increasing the stub bandwidth.

Using (1), (2), and (3), a transition was designed for optimum operation at 10.6 GHz with a maximum operating frequency as given in (3) of approximately 40 GHz. The stub length l was 1250 μm long, the stub inner radius r_1 was 125 μm, and the stub angle θ was 180°. The transition was fabricated on a semi-insulating GaAs substrate with a thickness of about 92 μm and a relative dielectric constant of about 12.9. The transitions were patterned in a 1.7-μm-thick layer of evaporated gold with a 500-Å-thick titanium adhesion layer using lift-off techniques. Alignment keys in the form of small 5 μm by 5 μm holes were printed on the radial stub as an aid in controlling the probe placement.

III. De-Embedding the Transition

While (1) is adequate for design purposes, it is not accurate enough to determine the electrical characteristics of the transition for purposes of de-embedding, as both the effects of fringing fields and circuit excitation were neglected in (1). Therefore an experimental procedure, referred to as unterminating [5], was used to electrically characterize the transition for purposes of de-embedding. Unterminating is the process of deducing the electrical characteristics of a transition from a series of S parameter measurements performed with known devices, which we will refer to as "standards," connected to the transition. The procedure used here is described in detail by Bauer and Penfield [5]. It is based on the fact that at any given frequency the transition is described by three complex S parameters (since the transition is reciprocal, $S_{12} = S_{21}$), and so three or more measurements performed with different "standards" connected to the transition are adequate for uniquely determining the S parameters of the transition.

The accuracy with which the S parameters of the transition can be determined is, for the most part, limited by the accuracy with which the "standards" have been characterized electrically. Microstrip loads are especially difficult to fabricate and characterize electrically. For this reason a set of planar offset microstrip opens were used as "standards." These offset opens are shown in Fig. 2. In order to electrically characterize these offset microstrip opens it was necessary to determine the attenuation constant α, the characteristic impedance Z_0, the propagation constant β, and the effective length extension l_{ext} (due to fringing capacitance at the end of the microstrip line) of the microstrip transmission lines.

The loss of the 90-μm-wide microstrip line was measured and the attenuation constant α found to be about 0.0053 nepers/mm at 17 GHz by comparing the return loss of several offset opens whose lengths differed by integer multiples of a half wavelength. (In this way, the effects of the transitions on the measurements was minimized.) The attenuation constant was then assumed to be proportional to the square root of the frequency, and was calculated from the measured loss at 17 GHz. This assumption is valid when the skin depth of the metal is much smaller than the metal thickness. This assumption breaks down at the lower end of the frequency range, but is a reasonable assumption above 10 GHz, where the calculated skin depth is 0.6 μm, about a third of the 1.7 μm metal thickness.

The dispersive characteristic impedance $Z_{0\text{lossless}}$ and the propagation constant β_{lossless} for the microstrip transmission lines were calculated by LINECALC [6] (which includes the effect of a finite metal thickness but neglects the effect of losses) at a set of

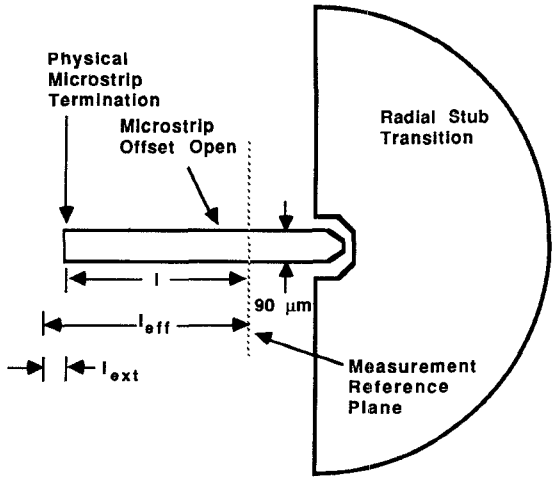

Fig. 2. Offset microstrip open "standards." The actual length l and the effective electrical length l_{eff} of these offset microstrip opens differ by the short length l_{ext}, as defined in the text, due to the excess capacitance of the microstrip open.

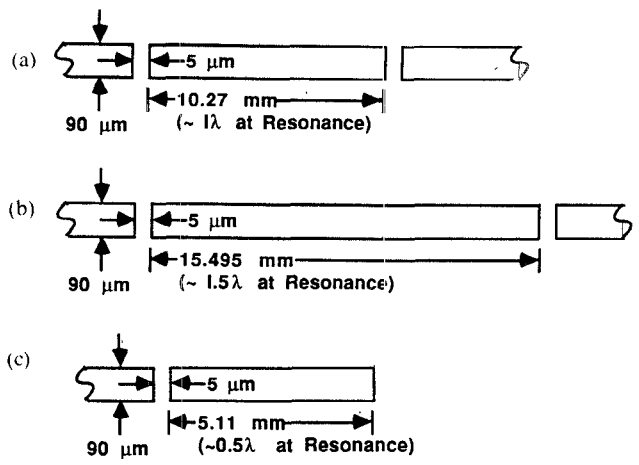

Fig. 3. Resonant structures for verifying the calculated propagation constant and effective length extension of the microstrip lines (a) A two-port resonator approximately one wavelength long at its resonant frequency of 9.846 GHz. (b) A two-port resonator identical to that in (a) but approximately one and a half wavelengths long at its resonant frequency of 9.83 GHz. (c) A one-port resonator approximately one half wavelength long at its resonant frequency of 9.845 GHz. The resonators in (b) and (c) were designed to resonate at the same frequency as the resonator in (a) The resonator in (b) was used to verify the calculated propagation constant. The resonator in (c) was used to verify the calculated value of l_{ext}.

discrete frequencies and then curve fitted. The lossless characteristic impedance and propagation constant were found to be well approximated by

$$Z_{0\text{lossless}} \approx k_0 + k_1 f + k_2 f^2 + k_3 f^3 \tag{4}$$

and

$$\beta_{\text{lossless}} = 2\pi\sqrt{\epsilon_{\text{eff}}}/\lambda_0 \tag{5}$$

where

$$\epsilon_{\text{eff}} \approx C_0 + C_1 f + C_2 f^2 + C_3 f^3$$

between 5 GHz and 25 GHz and where $k_0 = 43.2714\ \Omega$, $k_1 = -0.00635\ \Omega/\text{GHz}$, $k_2 = -0.000557\ \Omega/\text{GHz}^2$, $k_3 = 0.0000094\ \Omega/\text{GHz}^3$, $C_0 = 8.4009$, $C_1 = 0.00178\ \text{GHz}^{-1}$, $C_2 = 0.000295\ \text{GHz}^{-2}$, $C_3 = -0.00000445\ \text{GHz}^{-3}$, and f is the frequency. The actual impedance of the lossy line was then calculated from [7]

$$Z_0 = Z_{0\text{lossless}}\left(1 + (1-j)\,\alpha/\beta_{\text{lossless}}\right) \tag{6}$$

and the actual propagation constant β was calculated from [7]

$$\beta = \beta_{\text{lossless}}\left(1 + \alpha/\beta_{\text{lossless}}\right). \tag{7}$$

The propagation constant was checked experimentally by comparing the resonant frequencies of the two microstrip resonators shown in Fig. 3(a) and (b). These two resonators were identical except that the second was constructed to be half a wavelength longer at the resonant frequency of 9.84 GHz. This allowed the actual propagation constant to be easily calculated from the measured resonant frequencies (which should be identical if the propagation constant was calculated correctly) without knowing the exact electrical properties of the gap in the microstrip. The measured and calculated propagation constants were found to agree within the $\pm 0.3\%$ accuracy of the measurement.

As is well known [8], the fringing fields at the end of an open microstrip line give rise to an "excess" capacitance at the end of the line. This "excess" capacitance may be modeled electrically as an extension of the length of the line by a small amount, which we will call l_{ext}. This length extension was determined from an internal model for a microstrip open by the computer-aided design program TOUCHSTONE [6] to be $l_{ext} = 0.025$ mm. This value was verified with the resonant structure shown in Fig. 3(c). The length of the resonant section in Fig. 3(c) was chosen to be 0.025 mm less than one half of the length of the resonant section in Fig. 3(a) (which is just slightly less than one wavelength at the resonant frequency). At resonance there is a current null at the center of the resonator pictured in Fig. 3(a). Thus the resonant frequencies of the two circuits would be identical if l_{ext} were equal to its calculated value of 0.025 mm. This was found to be the case. This procedure allowed the verification of l_{ext} to within ± 0.015 mm, although the measurements were not accurate enough to correct for possible errors in the calculated value of l_{ext}.

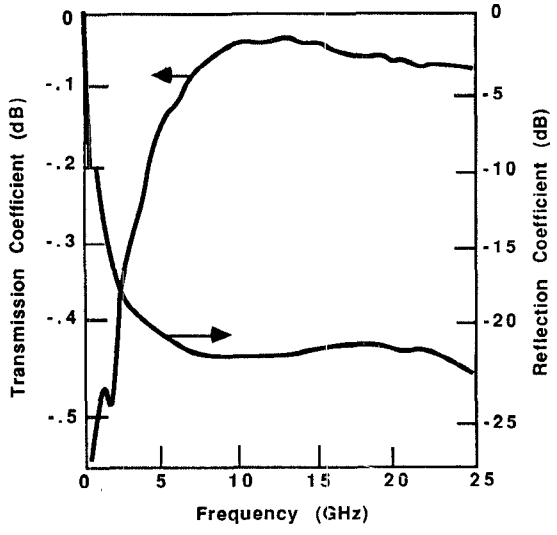

Fig. 4 The transmission and reflection coefficients of a single microstrip to coplanar probe transition are plotted. The S parameters of the transition were deduced by the unterminating procedure described in the text

Once the offset microstrip open "standards" had been characterized by the procedure described above, the transitions were unterminated. The analyzer and probe tips were first calibrated to a reference plane at the end of probe tips using planar standards provided by the manufacturer.[1] A set of 11 offset opens

[1]Impedance standard substrate ISS 12-39 manufactured by Cascade Microtech was used to calibrate the Cascade Microtech WPH-105-10 probe heads and the Hewlett Packard 8510 network analyzer as recommended by the manufacturer A Cascade Microtech manual probe station (model 42) was used for the measurements

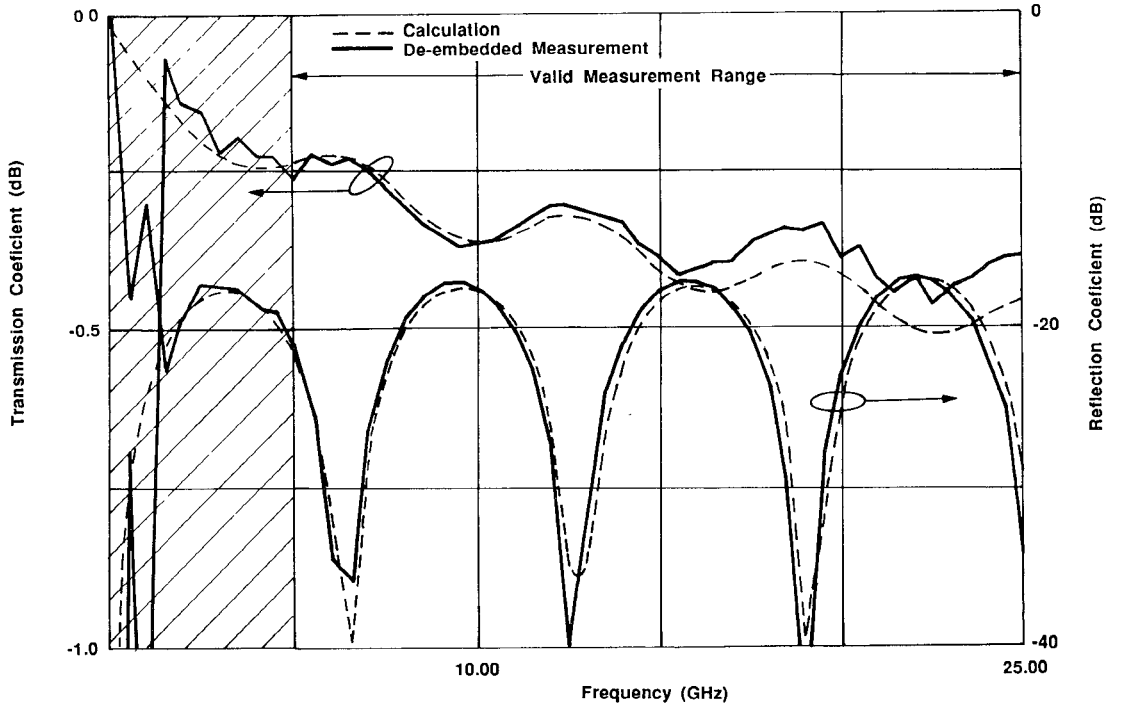

Fig 5 The calculated and de-embedded transmission and reflection coefficients of an 8-mm-long, 90-μm-wide microstrip transmission line on a 100-μm-thick GaAs substrate are compared. The discrepancy at low frequencies is caused in part by the lack of suitable standards and in part by the reduced coupling of the probe and microstrip grounds

TABLE I
ERRORS ESTIMATED FROM THE DE-EMBEDDED MEASUREMENTS OF MICROSTRIP OFFSET OPENS, MICROSTRIP THROUGH LINES, MICROSTRIP GAPS, AND THE MICROSTRIP RESONANT CIRCUITS SHOWN IN FIG. 3

Quantity	Estimated Error	Frequency (GHz)	Measurement Condition
Return Loss	±.1 dB ±.5°	5-15 GHz	$0 > \|S_{11}\| > 0.7$
	±.1 dB ±.2°	15-25 GHz	$0 > \|S_{11}\| > 0.7$
Transmission	±.05 In Magnitude	5-25 GHz	$0 > \|S_{11}\| > 0.7$
	±.1 dB ±.1°/GHz	5-15 GHz	$0 > \|S_{12}\| > 0.7$
	±.1 dB ±.1°/GHz	15-25 Ghz	$0 > \|S_{12}\| > 0.7$

with lengths of 0.5 mm, 1.0 mm, 1.5 mm, 2.0 mm, 3.0 mm, 4.0 mm, 5.0 mm, 6.0 mm, 7.0 mm, 8.5 mm, and 10.0 mm were then used as "standards" to unterminate the transition by performing a least-squares fit to the S parameters of the transition using the algorithm described by Bauer and Penfield [5]. The transmission coefficient of a single transition, determined by the unterminating process described above, is shown in Fig. 4. Referring to Fig. 4, a single transition is seen to have less than -0.15 dB transmission loss and greater than -20 dB return loss from 5 to 25 GHz, making them suitable for performing accurate S parameter measurements of microstrip circuits over more than two octaves.

IV. Measurement Verifications

De-embedded measurements of the offset microstrip open standards allow the determination of random measurement errors for large reflection coefficients. Systematic errors, such as those due to errors in the calculation of the characteristic impedance and effective dielectric constant of the microstrip lines used to fabricate the microstrip impedance standards, can not be easily estimated from measurements of these "standards." This is because the "standards are mapped into their definitions by the de-embedding process, even when four or more "standards" are used. In order to better estimate systematic measurement errors in the de-embedding and unterminating process, de-embedded measurements of single gaps in microstrip lines were used to predict the resonant frequencies, quality factors, and insertion losses of the resonant structures in Fig. 3(a) and (b). Comparisons of the actual resonant frequencies, quality factors, and insertion losses of these resonant structures with those derived from the de-embedded S parameter measurements of the gaps allow the measurement accuracy at high reflection coefficients and low transmission coefficients to be estimated. In this case, the differences between the measured and expected resonant frequencies are related to the error in the angle of the de-embedded reflection coefficients while differences between insertion loss and quality factors are related to the error in the magnitude of the de-embedded transmission coefficients. Measurements of microstrip through lines of different lengths (through lines were not used as standards in the de-embedding process) allowed estimates of measurement errors at low reflection coefficients and high transmission coefficients. In this case, the measured and expected transmission and reflection coefficients can be compared directly to estimate measurement error. Such a comparison for an 8-mm-long through line is shown in Fig. 5. Worst-case estimates of the de-embedded measurement errors so derived are listed in Table I.

V. Conclusions

A transition between a microstrip line and a coplanar probe suitable for measurements between 5 and 25 GHz was described. The transition was de-embedded and estimates of de-embedded

measurement accuracy performed. The high measurement accuracy obtained with these transitions allows coplanar probes to be used to test microstrip circuits without via holes at the wafer level. The need for mounting circuits in fixtures for testing is eliminated, resulting in lower testing costs.

The transition may prove especially useful at millimeter wavelengths, where its size can be reduced. Work to characterize this transition at millimeter wavelengths is in progress. Work to determine the S parameters of the transition as a function of substrate thickness is also in progress.

References

[1] K. E. Jones, E. W. Strid, and K. R. Gleason, "mm-wave wafer probes span 0 to 50 GHz," *Microwave J.*, vol. 30, no. 4, pp. 177–183, Apr. 1987.

[2] J. Moniz, "Modeling GaAs MMIC passive elements using RF probing," *GaAs Line*, vol. 1, no. 1, pp. 4–5, Mar. 1987.

[3] D. Harvey, "A lumped coplanar to microstrip transition model for de-embedding S-parameters measured on GaAs wafers," in *29th Automatic RF Tech. Group Conf. Proc.*, June 1987, pp. 204–217.

[4] H. A. Atwater, "Microstrip reactive circuit elements," *IEEE Trans. Microwave Theory Tech.*, vol. MTT-31, pp. 488–491, June 1983.

[5] R. F. Bauer and P. Penfield, "De-embedding and unterminating," *IEEE Trans. Microwave Theory Tech.*, vol. MTT-22, pp. 282–288, Mar. 1974.

[6] LINECALC and TOUCHSTONE were developed by and are trademarks of EEsof of Westlake, CA.

[7] S. Ramo, J. R. Whinnery, and T. Van Duzer, *Fields and Waves in Communication Electronics*, 2nd ed. New York: Wiley, 1984.

[8] P. Silvester and P. Benedek, "Equivalent capacitances of microstrip open circuits," *IEEE Trans. Microwave Theory Tech.*, vol. MTT-20, pp. 511–516, Aug. 1972.

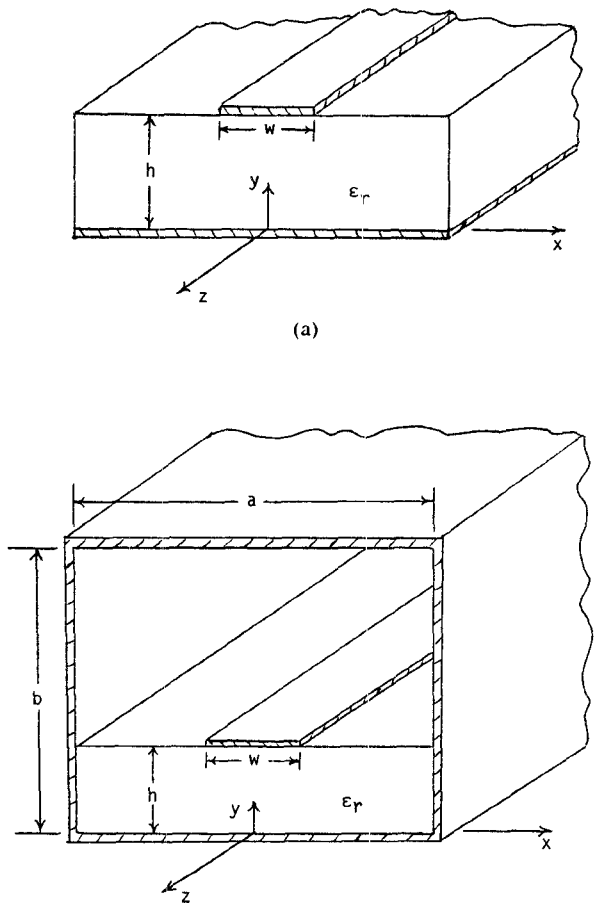

Fig. 1. Configuration and parameters of (a) open microstrip and (b) shielded microstrip lines.

Pulse Dispersion Distortion in Open and Shielded Microstrips Using the Spectral-Domain Method

TONY LEUNG, STUDENT MEMBER, IEEE, AND
CONSTANTINE A. BALANIS, FELLOW, IEEE

Abstract—**The spectral-domain method is used to compute the effective dielectric constant $[\epsilon_{r_{eff}}(f)]$ of open and shielded microstrip lines to analyze the dispersion distortion of short electrical pulses. Precise expressions for the longitudinal and transverse current distributions allow a high level of accuracy for $\epsilon_{r_{eff}}(f)$. It is determined that computation time can be minimized for the open microstrip calculations by using the shielded microstrip formulation provided large dimensions for the conducting walls are taken.**

I. Introduction

The analysis of the transient signal response in microstrip transmission lines is important in microwave integrated circuits (MIC's) when large-bandwidth signals or high switching speeds are considered. Electrical pulses generated from optoelectronic switching typically have wide spectra that extend into the dispersive frequency region of microstrip lines. In the past, transient signal behavior in microstrip lines was analyzed with quasi-static formulas for the effective dielectric constant, $\epsilon_{r_{eff}}(f)$, of the fundamental mode [1]–[5]. However, detailed pulse dispersion has not yet been examined with $\epsilon_{r_{eff}}(f)$ obtained from rigorous full-wave analyses such as the spectral-domain method [6], [7]. Neither have comparisons been made of distorted pulses using full-wave methods and quasi-static techniques.

This paper considers the dispersion of short electrical pulses propagating along open and shielded microstrip lines (Fig. 1) with $\epsilon_{r_{eff}}(f)$ calculated from the spectral-domain method. The accuracy of this method can be increased systematically by including more basis functions for the longitudinal and transverse currents ($J_z(x)$ and $J_x(x)$, respectively). However, as pointed out by Kobayashi, only one basis function for each current component is sufficient if these distributions are very good approximations of the exact currents on the strip conductor [8], [9]. Therefore the expressions for $J_z(x)$ and $J_x(x)$ considered in this paper are accurate formulas which allow the currents to be represented by only one basis function. This corresponds to the "first-order" solution of [6] and [7], while neglecting the transverse current corresponds to the "zero-order" solution. For comparison purposes, the zero- and first-order solutions are used to compute the dispersion curve of open and shielded microstrip lines. Also, the current expressions considered here will be used for both the open and the shielded lines so that their dispersive characteristics may be compared. It is shown that computation time may be minimized by using the shielded line formulation for the open line calculations. Finally, pulses calculated with $\epsilon_{r_{eff}}(f)$

Manuscript received November 16, 1987; revised February 20, 1988. This work was supported by the U.S. Army Research Office under Contract DAAG29-85-K-0078.

T. Leung was with the Department of Electrical and Computer Engineering, Arizona State University, Tempe, AZ. He is now with the Aerospace Corporation, 200 N. Aviation Blvd., El Segundo, CA 90245.

C. A. Balanis is with the Department of Electrical and Computer Engineering, Arizona State University, Tempe, AZ 85287.

IEEE Log Number 8821227.